Au Nanoparticle-based Multilayer Ultrathin Films with Covalently Linked Nanostructures: Spraying Layer-by-layer Assembly and Mechanical Property Characterization

Conghua Lu, Ingo Dönch, Marc Nolte, and Andreas Fery*

Interface Department, Max Planck Institute of Colloids and Interfaces, 14424 Potsdam, Germany

Received July 27, 2006. Revised Manuscript Received October 16, 2006

We have studied electrostatic layer-by-layer spraying assembly of inorganic/organic nanocomposite multilayered films consisting of Au nanoparticle (Au NP) and photosensitive polycation nitrodiazoresin (NDR). A uniform growth of the Au NP-based assembly film is revealed by UV−vis spectroscopy and AFM-film thickness measurements. We demonstrate that cross-linked films can be produced by UV irradiation which induces the conversion of originally ionic bonds into covalent ones. The nanostructure of the film such as the thickness and the fraction of Au NP can be tailored by the adsorption conditions. Thus, we find that the mechanical properties, which were measured using a buckling test method, can be tailored to a certain degree.

Introduction

Integration of functional inorganic nanoparticles (NPs) into organic matrixes to form organized inorganic/organic hierarchical ultrathin films with well-defined nanostructures has attracted extensive interest due to their broad applications,[1] for example, Au NP-based ultrathin films have potential in the areas of advanced microelectronic devices, nonlinear optics, electrochemical sensor and bioanalysis, and so forth.[2,3] Recently, increasing attention has been paid to the reinforcement of inorganic NPs on the mechanical properties of the resulting nanocomposite films,[3−5] which are well related with their potential applications.[6,7] It is reminiscent of natural inorganic/organic hierarchical composites with the representative example of abalone nacre,[8] which has inspired materials scientists to exploit the basic principle to biomimetically synthesize advanced materials.[3−5,9] So far, magnetite nanoparticles,[5a] montmorillonite clay nanoplatelets,[5a,c] Au NPs,[3] and carbon nanotubes[5b,d,10] have been incorporated into composite films, resulting in extraordinary mechanical properties, as well as superior sensitivity and autorecovery capability. However, systematic research on the effect of inorganic NPs on the mechanical properties still lacks, and the reinforcement mechanism is not fully clear yet.

Introduction of inorganic NPs to form ordered inorganic/organic hybrid ultrathin films (or membranes) can be realized through self-assembly or in-situ synthesis of inorganic NPs in polymer templates[11,12] and polyelectrolytes (PEs) multilayer nanoreactors,[13] Langmuir−Blodgett deposition,[14] or the well-established layer-by-layer (LbL) self-assembly of inorganic NPs.[1b,d 2c,d 3−5,15−17] It is well-known that the LbL

* To whom correspondence may be addressed. E-mail: andreas.fery@mpikg.mpg.de. Tel: +49-(0)-331-5679204. Fax: +49-(0)-331-5679202.

(1) (a) Mattoussi, H.; Radzilowski, L. H.; Dabbousi, B. O.; Thomas, E. L.; Bawendi, M. G.; Rubner, M. F. *J. Appl. Phys.* **1998**, *83*, 7965. (b) Aliev, F. G.; Correa-Duarte, M. A.; Mamedov, A.; Ostrander, J. W.; Giersig, M.; Liz-Marzan, L. M.; Kotov, N. A. *Adv. Mater.* **1999**, *11*, 1006. (c) Vossmeyer, T.; Guse, B.; Besnard, I.; Bauer, R. E.; Mullen, K.; Yasuda, A. *Adv. Mater.* **2002**, *14*, 238. (d) Park, J.; Fouche, L. D.; Hammond, P. T. *Adv. Mater.* **2005**, *17*, 2575.

(2) (a) Elghanian, R.; Storhoff, J. J.; Mucic, R. C.; Letsinger, R. L.; Mirkin, C. A. *Science* **1997**, *277*, 1078. (b) He, L.; Musick, M. D.; Nicewarner, S. R.; Salinas, F. G.; Benkovic, S. J.; Natan, M. J.; Keating, C. D. *J. Am. Chem. Soc.* **2000**, *122*, 9071. (c) Gittins, D. I.; Susha, A. S.; Schoeler, B.; Caruso, F. *Adv. Mater.* **2002**, *14*, 508. (d) Yu, A.; Liang, Z.; Cho, J.; Caruso, F. *Nano Lett.* **2003**, *3*, 1203. (e) Daniel, M.-C.; Astruc, D. *Chem. Rev.* **2004**, *104*, 293.

(3) (a) Jiang, C.; Markutsya, S.; Pikus, Y.; Tsukruk, V. V. *Nat. Mater.* **2004**, *3*, 721. (b) Jiang, C.; Markutsya, S.; Tsukruk, V. V. *Adv. Mater.* **2004**, *16*, 157. (c) Jiang, C.; Markutsya, S.; Tsukruk, V. V. *Langmuir* **2004**, *20*, 882. (d) Jiang, C.; Markutsya, S.; Shulha, H.; Tsukruk, V. V. *Adv. Mater.* **2005**, *17*, 1669. (e) Markutsya, S.; Jiang, C.; Pikus Y.; Tsukruk, V. V. *Adv. Funct. Mater.* **2005**, *15*, 771. (f) Jiang, C.; McConney, M. E.; Singamaneni, S.; Merrick, E.; Chen, Y.; Zhao, J.; Zhang, L.; Tsukruk, V. V. *Chem. Mater.* **2006**, *18*, 2632. (g) Jiang, C.; Tsukruk, V. V. *Adv. Mater.* **2006**, *18*, 829.

(4) Aksay, I. A.; Trau, M.; Manne, S.; Honma, I.; Yao, N.; Zhou, L.; Fenter, P.; Eisenberger, P. M.; Gruner, S. M. *Science* **1996**, *273*, 892.

(5) (a) Mamedov, A. A.; Kotov, N. A. *Langmuir* **2000**, *16*, 5530. (b) Mamedov, A. A.; Kotov, N. A.; Prato, M.; Guldi, D. M.; Wicksted, J. P.; Hirsch, A. *Nat. Mater.* **2002**, *1*, 190. (c) Tang, Z.; Kotov, N. A.; Magonov, S.; Ozturk, B. *Nat. Mater.* **2003**, *2*, 413. (d) Olek, M.; Ostrander, J.; Jurga, S.; Möhwald, H.; Kotov, N.; Kempa, K.; Giersig, M. *Nano Lett.* **2004**, *4*, 1889.

(6) Thompson, M. T.; Berg, M. C.; Tobias, I. S.; Rubner, M. F.; Van Vliet, K. J. *Biomaterials* **2005**, *26*, 6836.

(7) Gupta, S.; Zhang, Q.; Emrick, T.; Balazs, A. C.; Russell, T. P. *Nat. Mater.* **2006**, *5*, 229.

(8) Smith, B. L.; Schaffer, T. E.; Viani, M.; Thompson, J. B.; Frederick, N. A.; Kindt, J.; Belcher, A.; Stuckyk, G. D.; Morse, D. E.; Hansma, P. K. *Nature* **1999**, *399*, 761.

(9) Sanchez, C.; Arribart, H.; Guille, M. M. G. *Nat. Mater.* **2005**, *4*, 277.

(10) (a) Ko, H.; Jiang, C.; Shulha, H.; Tsukruk, V. V. *Chem. Mater.* **2005**, *17*, 2490. (b) Jiang, C.; Ko, H. Y.; Tsukruk, V. V. *Adv. Mater.* **2005**, *17*, 2127.

(11) Vendamme, R.; Onoue, S. Y.; Nakao, A.; Kunitake, T. *Nat. Mater.* **2006**, *5*, 494.

(12) Lin, Y.; Boker, A.; He, J.; Sill, K.; Xiang, H.; Abetz, C.; Li, X.; Wang, J.; Emrick, T.; Long, S.; Wang, Q.; Balazs, A.; Russell, T. P. *Nature* **2005**, *434*, 55.

(13) (a) Joly, S.; Kane, R.; Radzilowski, L.; Wang, T.; Wu, A.; Cohen, R. E.; Thomas, E. L.; Rubner, M. F. *Langmuir* **2000**, *16*, 1354. (b) Shia, X.; Shen, M.; Möhwald, H. *Prog. Polym. Sci.* **2004**, *29*, 987. (c) Shchukin, D. G.; Sukhorukov, G. B. *Adv. Mater.* **2004**, *16*, 671.

(14) Chen, S. *Langmuir* **2001**, *17*, 2878.

(15) (a) Decher, G. *Science* **1997**, *277*, 1232. (b) Decher, G. *Polyelectrolyte multilayers−−−an overview, in Multilayer thin films: Sequential assembly of nanocomposite materials*; Decher, G., Schlenoff, J. B., Eds.; Wiley-VCH: Weinheim, Germany, 2002, pp 1−46.

10.1021/cm061759y CCC: $33.50
Published on Web 12/06/2006

assembly is based on alternating adsorption of oppositely charged polyions on charged substrates to build up multilayered composite films with controlled nanostructures.[15,17] So far, a variety of functional inorganic building blocks have been integrated, exploiting driving forces such as electrostatic interaction, hydrogen bonding, and charge transfer.[3−5,15−18] Whereas, construction of monolayer and multilayer films using classical dipping procedures is rather time-consuming (typically 30 min per dipping cycle). Recently, other two efficient, alternative assembly techniques have been developed, that is, spinning-assisted assembly[19] and spraying assembly.[20,21] Thus, spraying buildup of PEs multilayers with conveniently tailorable nanostructures can be accelerated by 1−2 orders of magnitude in comparison with the familiar dipping assembly while the quality of the films is equal or superior.[21b] To our knowledge, however, there are few reports about fabrication of inorganic NP-related spraying film and it may be more advantageous to efficiently construct NP multilayers via the above spraying assembly.

On the other hand, the processing and the applications of multilayer ultrathin films are well related to the mechanical properties and chemical stability. Thereby, understanding how to improve the stability of the assembled films is essential because the assembled films are linked mainly by ionic bonds and other noncovalent interactions. Naturally, introduction of stable covalent cross-linkages into the assembled layers is a feasible method to address it, such as thermal treatment,[22] addition of coupling reagents,[23] or UV irradiation of photosensitive diazoresin (DR) or nitrodiazoresin (NDR)-based assembly films.[24−26] The formation of covalent cross-links not only enhances the chemical stability and mechanical properties of the nanocomposite films but also imparts the films other properties such as good ion-transport selectivity and well-tuned release rate of encapsulated drugs or molecules.[22a]

Recently, DR (or NDR)-based multilayer composite films including functional Au NP as one component have been constructed with the familiar dipping assembly and their chemical stabilities and photocross-linking reaction except the mechanical properties have been well investigated.[24−26] In this paper, covalently cross-linked NDR/Au NP multilayer films with controlled nanostructures have been further efficiently fabricated by spraying LbL assembly. The effect of assembled film structures on the mechanical properties have been quantitatively investigated with a recently developed method based on buckling instabilities of supported films.[27]

Experimental Section

1. Materials. Poly(sodium 4-styrene sulfonate) (PSS, $M_w \sim 100\,000$), poly(diallyldimethyl ammonium chloride) (PDDAC, $M_w \sim 100\,000-200\,000$), and poly(ethylenimine) (PEI, $M_w \sim 25\,000$) were purchased from Sigma-Aldrich and used without purification. Nitrodiazoresin (NDR, $M_n \sim 2100$ g/mol) presented by Prof. Weixiao Cao (Peking University, Beijing, China) was synthesized from 2-nitro-*N*-methyldiphenylamine-4-diazonium salt with paraformaldehyde in concentrated sulfuric acid.[28] Approximately 5-nm-sized Au nanoparticles (Au NPs) were prepared by borohydride reduction in the presence of trisodium citrate.[29] Briefly, at room temperature, 0.6 mL of ice-cold freshly prepared 0.1 M $NaBH_4$ solution was added to 20 mL mixed solutions composed of equal molar 2.5×10^{-4} M $HAuCl_4$ and trisodium citrate, accompanied by strong stirring. After 10 min of continuous stirring, the obtained Au NP solution was adjusted to pH = 7.5 with 1 M HCl and then kept at 4 °C for later spraying assembly. PSS, PDDAC, and NDR were dissolved in Milli-Q water (the resistivity was higher than 18 MΩ·cm) with a concentration of 0.5 mg/mL, respectively. A mixed solution composed of 0.5 mg/mL of PSS and 2.5×10^{-4} M Au NPs or composed of 0.5 mg/mL of PDDAC and 0.25 mg/mL of NDR was also prepared.

The substrates of silicon wafer, glass, and quartz slides were cleaned following the RCA protocol:[30] sonication in a mixture of 3:1 (vol %) H_2O/isopropanol for 15 min and then immersion in 5:1:1 (vol %) $H_2O/H_2O_2/NH_3$ mixed solution at 70 °C for 10 min, followed by thoroughly washing with Milli-Q water.

A poly(dimethylsiloxane) (PDMS) sheet with thickness ~1 mm was prepared by mixing the curing agent and base monomer (Sylgard 184, Dow Corning) at a 1:10 ratio (by mass) and casting into a tray.[31] After the mixture was degassed for 30 min, it was baked at 60 °C for 12 h. To obtain a hydrophilic surface, the PDMS sheet was treated with air plasma (Harrick PDC 32G) in 0.02 mbar pressure with low intensity for 1 min and then immersed in 1 mg/mL PEI solution for later assembly.

2. Spraying Layer-by-Layer Assembly of Ultrathin Film on Different Substrates. Spraying assembly of polyelectrolyte multilayered films was carried out through alternate spraying of

(16) Liu, Y.; Wang, Y.; Claus, R. O. *Chem. Phys. Lett.* **1998**, *298*, 315.
(17) Bertrand, P.; Jonas, A.; Laschewsky, A.; Legras, R. *Macromol. Rapid Commun.* **2000**, *21*, 319.
(18) Crespo-Biel, O.; Dordi, B.; Reinhoudt, D. N.; Huskens, J. *J. Am. Chem. Soc.* **2005**, *127*, 7594.
(19) (a) Chiarelli, P. A.; Johal, M. S.; Casson, J. L.; Roberts, J. B.; Robinson, J. M.; Wang, H.-L. *Adv. Mater.* **2001**, *13*, 1167. (b) Cho, J.; Char, K.; Hong, J.-D.; Lee, K.-B. *Adv. Mater.* **2001**, *13*, 1076.
(20) Schlenoff, J. B.; Dubas, S. T.; Farhat, T. *Langmuir* **2000**, *16*, 9968.
(21) (a) Porcel, C. H.; Izquierdo, A.; Ball, V.; Decher, G.; Voegel, J.-C.; Schaaf, P. *Langmuir* **2005**, *21*, 800. (b) Izquierdo, A.; Ono, S. S.; Voegel, J.-C.; Schaaf, P.; Decher, G. *Langmuir* **2005**, *21*, 7558. (c) Ono, S. S.; Decher, G. *Nano lett.* **2006**, *6*, 592.
(22) (a) Dai, J.; Jensen, A. W.; Mohanty, D. K.; Erndt, J.; Bruening, M. L. *Langmuir* **2001**, *17*, 931. (b) Mallwitz, F.; Laschewsky, A. *Adv. Mater.* **2005**, *17*, 1296.
(23) (a) Huck, W. T. S.; Stroock, A. D.; Whitesides, G. M. *Angew. Chem., Int. Ed.* **2000**, *39*, 1058. (b) Stroock, A. D.; Kane, R. S.; Weck, M.; Whitesides, G. M. *Langmuir* **2003**, *19*, 2466. (c) Li, Q.; Quinn, J. F.; Caruso, F. *Adv. Mater.* **2005**, *17*, 2058. (d) Lutkenhaus, J. L.; Hrabak, K. D.; McEnnis, K.; Hammond, P. T. *J. Am. Chem. Soc.* **2005**, *127*, 17228.
(24) Pastoriza-Santos, I.; Scholer, B.; Caruso, F. *Adv. Funct. Mater.* **2001**, *11*, 122.
(25) (a) Sun, J.; Wu, T.; Sun, Y.; Wang, Z.; Zhang, X.; Shen, J.; Cao, W. X. *Chem. Commun.* **1998**, 1853. (b) Sun, J.; Wu, T.; Liu, F.; Wang, Z.; Zhang, X.; Shen, J. *Langmuir* **2000**, *16*, 4620. (c) Shi, F.; Dong, B.; Qiu, D.; Sun, J.; Wu, T.; Zhang, X. *Adv. Mater.* **2002**, *14*, 805. (d) Fu, Y.; Xu, H.; Bai, S.; Qiu, D.; Sun, J.; Wang, Z.; Zhang, X. *Macromol. Rapid Commun.* **2002**, *23*, 256.
(26) (a) Chen, J.; Huang, L.; Ying, L.; Luo, G.; Zhao, X.; Cao, W. *Langmuir* **1999**, *15*, 7208. (b) Lu, C.; Wu, N.; Jiao, X.; Luo, C.; Cao, W. *Chem. Commun.* **2003**, 1056. (c) Lu, C.; Wu, N.; Wei, F.; Zhao, X.; Jiao, X.; Xu, J.; Luo, C.; Cao, W. *Adv. Funct. Mater.* **2003**, *13*, 548. (d) Lu, C.; Wei, F.; Wu, N.; Huang, L.; Zhao, X.; Luo, C.; Cao, W. *Langmuir* **2004**, *20*, 974.
(27) (a) Stafford, C. M.; Harrison, C.; Beers, K. L.; Karim, A.; Amis, E. J.; Vanlandingham, M. R.; Kim, H. C.; Volksen, W.; Miller, R. D.; Simonyi, E. E. A. *Nat. Mater.* **2004**, *3*, 545. (b) Wilder, E. A.; Guo, S.; Lin-Gibson, S.; Fasolka, M. J.; Stafford, C. M. *Macromolecules* **2006**, *39*, 4138. (c) Stafford, C. M.; Vogt, B. D.; Harrison, C.; Julthongpiput, D.; Huang, R. *Macromolecules* **2006**, *39*, 5095.
(28) Wang, R.; Chen, J.; Cao, W. *J. Appl. Polym. Sci.* **1999**, *74*, 189.
(29) Jana, N. R.; Gearheart, L.; Murphy, C. J. *Langmuir* **2001**, *17*, 6782.
(30) Kern, W. *Semicond. Int.* **1984**, 94.
(31) Nolte, M.; Schoeler, B.; Peyratout, C. S.; Kurth, D. G.; Fery, A. *Adv. Mater.* **2005**, *17*, 1665.

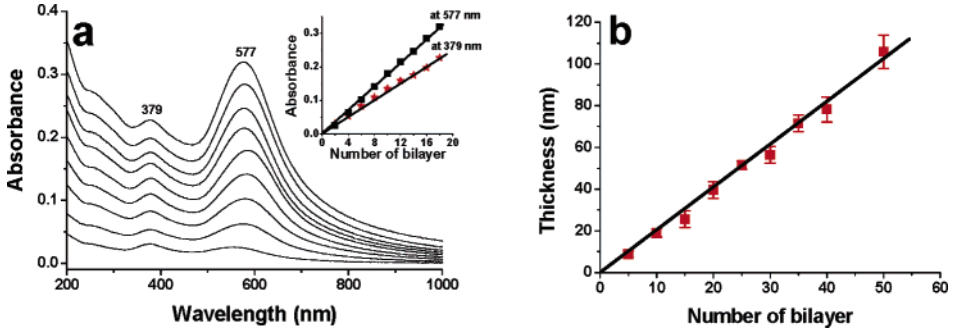

Figure 1. UV−vis absorption spectra (a) and the thickness (b) of as-prepared NDR/Au NP multilayer film with different deposition cycles on a quartz slide. The absorption of the substrate has been subtracted. The inset in plate a shows a linear relationship between the absorbances at 379 and 577 nm with the number of deposited bilayers, respectively.

assembly solutions on a perpendicular substrate with spray bottles "air-boy" (Carl Roth GmbH, Germany) as described in ref 21b. In our case, some modifications have been made for the inorganic NP composite films. Here NDR/Au NP assembly film was taken as one sample. Initially, NDR aqueous solution was sprayed for two sequential times (3 s duration each) with 10 s waiting time after each time's spraying, followed by 5 s water washing and subsequent 10 s waiting; then, the Au NP solution was sprayed for another sequential 4 times (3 s duration each) while also inserting 10 s of waiting time after each time's spraying assembly, accompanied by the same time's water rinsing and waiting in air. So, the total time to deposit one NDR/Au NP bilayer is about 2 min. $(NDR/Au\ NP)_n$ multilayers with a desirable number (n) of bilayers are obtained after simply repeating the above spraying assembly cycles for n times. It should be noted that illumination of the photosensitive film during the whole assembly process should be avoided because of the photosensitive polycation of NDR.

3. Characterization. UV−vis spectroscopy was carried out on a CARY 50 Conc (Varian) spectrophotometer after completion of each assembly cycle on a quartz slide, and an air blank was taken for all the measurements. The photoreaction occurring in the film upon UV irradiation was also determined spectroscopically. Atomic force microscopy (AFM) images were obtained using a NanoWizard AFM (JPK Instrument, Berlin) operating in tapping mode with silicon cantilevers (NC−W, the typical frequency of 285 kHz). Transmission electron microscopy (TEM) was performed on a Zeiss EM 912 Omega microscope with an accelerating voltage of 120 kV. For the buckling test, the multilayered film was directly deposited on a plasma-treated PDMS sheet with the above spraying assembly method.[32a] Then the PDMS sheet with UV-irradiated film coated on its surface was subjected to strain with small deformation and then fixed by two clamps with a relative humidity of ∼40−50%. The resultant regular ridges during the buckling test were observed and recorded by a charge coupled device (CCD) camera equipped on an optical microscope (Axiovert 200, Zeiss). The buckling wavelength was calculated and averaged without Fourier transform. The Young's modulus of the PDMS sheet was determined on a homemade microtensile testing device.[33]

Results and Discussion

The as-prepared Au NPs with ∼5 nm diameter and the typical surface plasmon resonance (SPR) absorption at 512 nm (Figure S1) have negative surface charges due to the citrate ion as the surface capping and stabilizing agent. Therefore, self-assembly of Au NP-based multilayer films can be readily driven via electrostatic interactions. Here, we utilized the spraying-assisted assembly to construct the composite film. In contrast to previous studies,[20,21] where mainly PEs were assembled, the embedding of nanoparticles requires optimizing the spraying assembly parameters. The preparation of the NDR monolayer was carried out just as shown in the experimental section; for subsequent Au NP layer, we mainly investigated the effect of spraying manners such as the spraying time (i.e., spraying cycles) and the waiting time on the buildup of Au NP layer, while the rinsing step has not been studied in detail in view of the excessive components continuously removed by the drainage.[21b] It is found that the deposited amount of Au NPs increases with simply repeated spraying of Au NP solution, which is different from the reported results of PE films that PE monolayer thickness is not influenced by the spraying cycles of the same polyions without intermediate rinsing.[21b] Furthermore, four times sequential spraying assembly seems better with good coverage of Au NPs on an underlying NDR layer and no obvious aggregation. Higher spraying times such as 8 and 24 times result in multilayer absorption of Au NPs with some aggregation. Additionally, a minimal delay time of 10 s between spraying cycles needs to be used to obtain a good quality Au NP layer. Therefore, in the following experiment, we sprayed Au NP solution successively 4 times with 10 s waiting after each time's spraying to deposit the Au NP monolayer.

UV−vis spectroscopy was used to monitor the assembly process of NDR/Au NP multilayer film on a quartz glass (Figure 1a). The appearance of the characteristic $\pi-\pi^*$ transition of N_2^+ absorption at 379 nm in the UV−vis spectra indicates the successive incorporation of NDR into the composite film.[25,26] Here, there exists a red shift of ∼65 nm for the typical SPR absorption peak of Au NP from 512 nm of an Au NP solution (Figure S1) to the final 577 nm of the composite film (Figure 1a). This may be attributed to the reduction in distance between neighboring Au NPs in the assembly film as compared with Au NP in aqueous solution,[34a−c] the change of the refractive index of the

(32) (a) Nolte, A. J.; Rubner, M. F.; Cohen, R. E. *Macromolecules* **2005**, *38*, 5367. (b) Nolte, A. J.; Cohen, R. E.; Rubner, M. F. *Macromolecules* **2006**, *39*, 4841.
(33) Burgert, I.; Frühmann, K.; Keckes, J.; Fratzl, P.; Stanzl-Tschegg, S. E. *Holzforschung* **2003**, *57*, 661.
(34) (a) Mirkin, C. A.; Letsinger, R. L.; Mucic, R. C.; Storhoff, J. J. *Nature* **1996**, *382*, 607. (b) Brust, M.; Bethell, D.; Kiely, C. J.; Schiffrin, D. J. *Langmuir* **1998**, *14*, 5425. (c) Schmitt, J.; Mächtle, P.; Eck, D.; Möhwald, H.; Helm, C. A. *Langmuir* **1999**, *15*, 3256. (d) Schneider, G.; Decher, G. *Nano Lett.* **2004**, *4*, 1833.

Scheme 1. Schematic Illustration of the Bond Conversion in the NDR/Au NP Multilayer Film under UV Irradiation.

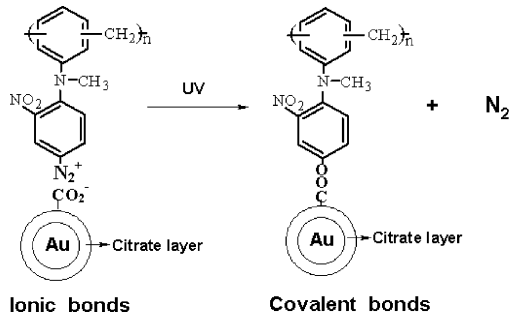

surrounding PE matrix,[3c,34c,d] or interparticle bridging and aggregation of Au NPs.[25d,34c,d] The latter aggregation behavior of NPs occurs commonly in the NP-containing composite assembly films.[34d] It is pointed out that the red shift appears quickly on the first four bilayers and later almost remains constant with the increase in the film thickness, implying a uniform separation and distribution of Au NPs during the later buildup process.[2d,35] The linear increase in the absorbance at 379 and 577 nm with the number of assembled bilayers is indicative of the regular growth of NDR and Au NP in the composite film, respectively. Additionally, AFM cross-section analysis of scratched films shows a linear dependence of the film thickness on the number of bilayers (Figure 1b). The thickness for the contribution of each NDR/Au NP bilayer is approximately 2 nm, smaller than the total value of monolayer polyelectrolyte (the increment is typically ~2 nm per bilayer) and Au NP (~5 nm in diameter). This results from some interpenetration between adjacent assembly layers[15−17,36] and low coverage (<30%) of inorganic NP on the PE layer after each deposition cycle.[37]

When the photosensitive multilayer film was exposed to UV light, the photodecomposition of NDR results in the decrease of absorption at 379 nm (part a of Figure S2). Meanwhile, the ionic bonds between NDR and citrate-capped Au NP layers were converted into covalent ones, just as schematically shown in Scheme 1. This kind of bond change from the original ionic bonds (−Ph−N_2^+/−CO_2^-) into the final covalent carboxylate ester (−Ph−OCO−) has been supported and well characterized by the corresponding recorded FTIR.[25b,26a] As a result, a covalently cross-linked composite film is formed with improved chemical stability.[24−26] Namely, an electrostatic-interaction-bonded film is easily damaged or dissolved in the testing media such as polar solvents (e.g., *N*,*N*-dimethylformamide (DMF)), concentrated salty solutions, and the typical ternary mixture of H_2O/DMF/LiCl. While under the same testing conditions, the UV-exposed film is stable and can keep intact. Furthermore, utilizing the distinct stability in an appropriate developer such as SDS solution, covalently linked films with well-defined micropatterns including inorganic NPs incorporated have been generated when the unirradiated part linked by ionic bonds or hydrogen bonding is dissolved by the developer while the stable covalently linked part produced by selective UV irradiation is reserved on the substrate.[25c,26b−e]

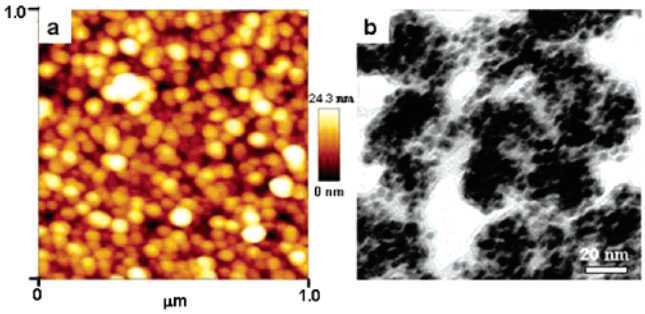

Figure 2. AFM (a) and TEM (b) images of a NDR/Au NP film transferred onto a copper grid after acetone dissolution of the cellulose acetate sacrificial layer.

When the composite film was deposited on a cellulose acetate (CA)-coated substrate, the UV-irradiated film can be transferred onto other substrates (e.g., a copper grid) after dissolution of the sacrificial CA layer in acetone.[3a,b,d−f, 5a,c] From the AFM image shown in Figure 2a, it is easy to see the transferred film with a root-mean-square (rms) roughness of 4.8 nm is composed of NPs with a diameter of 50−70 nm, obviously bigger than that of the Au NP (~5 nm, Figure S1). It is known that the AFM tip dilation usually adds 30−40% to the diameter of the NP.[2d,34c] In our case, however, it is not very critical as compared with the TEM data. Indeed, each NP with a comparable size consists of tens of ~5-nm-sized Au NPs with a darker contrast, surrounded by distinctive organic counterparts with a lighter contrast in the bright field of the TEM image (Figure 2b). Au NPs are aggregated through the linkage of organic components into bigger clusters, also further supporting the above explanation on the red shift of the SPR absorption for the deposited Au NP in the assembly films.

In the following, we have investigated how composition and structure of the film can be tailored. As expected for a layer-by-layer assembly, the thickness of the film can be controlled by simply changing spraying assembly cycles (i.e., number of bilayers) (Figure 1b). Interestingly, the composition of the organic and inorganic phases can be adjusted by using mixed solutions of the same charged polyions.[23c,38] For example, a blend solution composed of 0.5 mg/mL PDDAC and 0.25 mg/mL NDR results in the as-prepared (NDR + PDDAC)/Au NP film with an organic matrix of ~90 wt % NDR and 10 wt % PDDAC (parts a and b of Figure 3). This can be roughly estimated from traced UV spectroscopy (Figure 3a), when it is assumed that the contribution to the absorption at 379 and 578 nm in the UV−vis spectra comes from NDR and Au NP, respectively. Meanwhile, the covalent

(35) Cho, J. H.; Caruso, F. *Chem. Mater.* **2005**, *17*, 4547.
(36) (a) Correa-Duarte, M. A.; Giersig, M.; Kotov, N. A.; Liz-Marzán, L. M. *Langmuir* **1998**, *14*, 6430. (b) Baur, J. W.; Rubner, M. F.; Reynolds, J. R.; Kim, S. *Langmuir* **1999**, *15*, 6460. (c) Mamedov, A.; Ostrander, J.; Aliev, F.; Kotov, N. A. *Langmuir* **2000**, *16*, 3941.
(37) (a) Schmitt, J.; Decher, G.; Dressick, W. J.; Brandow, S. L.; Geer, R. E.; Shashidhar, R.; Calvert, J. M. *Adv. Mater.* **1997**, *9*, 61. (b) Musick, M. D.; Keating, C. D.; Lyon, L. A.; Botsko, S. L.; Pena, D. J.; Holliway, W. D.; McEvoy, T. M.; Richardson, J. N.; Natan, M. J. *Chem. Mater.* **2000**, *12*, 2869. (c) Ung, T.; Liz-Marzan, L. M.; Mulvaney, P. *J. Phys. Chem. B* **2001**, *105*, 3441.
(38) (a) Debreczeny, M.; Ball, V.; Boulmedais, F.; Szalontai, B.; Voegel, J.-C.; Schaaf, P. *J. Phys. Chem. B* **2003**, *107*, 12734. (b) Sui, Z.; Schlenoff, J. B. *Langmuir* **2003**, *19*, 7829. (c) Cho, J. H.; Quinn, J. F.; Caruso, F. *J. Am. Chem. Soc.* **2004**, *126*, 2270. (d) Johal, M. S.; Ozer, B. H.; Casson, J. L.; John, A. S.; Robinson, J. M.; Wang, H.-L. *Langmuir* **2004**, *20*, 2792. (e) Yap, H. P.; Quinn, J. F.; Ng, S. M.; Cho, J. H.; Caruso, F. *Langmuir* **2005**, *21*, 4328.

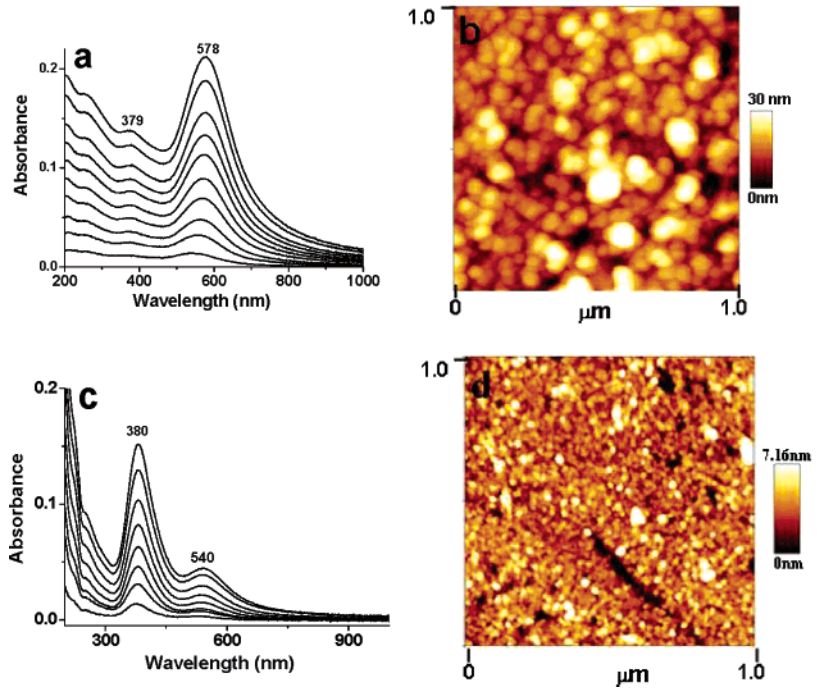

Figure 3. The evolution of UV−vis spectra (parts a and c) with the assembly process and AFM images (parts b and d) of hybrid films with controlled compositions: (a, b) $[(NDR + PDDAC)/Au\ NP]_{20}$; (c, d) $[NDR/(PSS + Au\ NP)]_{16}$. In the UV−vis absorption spectra, the absorbance of the quartz substrate has been subtracted.

cross-linkage density can also be adjusted because of the coexistence of the ionic bonds between PDDAC and Au NP with the covalent bonds after UV irradiation (Figure S2b). While the coexistence of 0.5 mg/mL PSS in the Au NP solution leads to ∼20% coverage of Au NP and ∼80% coverage replaced by PSS in the anionic assembled layers (parts c and d of Figure 3). It is maybe originated from the competitive interaction between the same negatively charged Au NP and PSS with cationic NDR. More importantly, just as the reported ligand of 4-(dimethylamino)pyridine for citrated-coated Au NP,[2c,d,39] PSS as a good capping agent replaces the weak capping agent of citrate[29] and adsorbs on the surface of Au NP to electrostatically interact with NDR. Consequently, the resulting film has a small rms roughness of 1.43 nm (Figure 3d). This explanation is confirmed by monitored UV−vis spectroscopy that the SPR absorption of Au NP solution in the presence of PSS occurs at 542 nm with ∼30 nm red shift, compared with Au NP solution without PSS added. Additionally, the SPR absorption peak (542 nm) almost agrees with that (540 nm) of the Au NP in the assembly film, suggesting Au NP in the PSS-coexisting solution and NDR/(PSS + Au NP) assembly film with the similar states (e.g., the refractive index of surrounding media). Naturally, compared with the red shift of the Au NPs' SPR absorption in the NDR/Au NP (Figure 1a) and (NDR + PDDAC)/Au NP multilayer films (Figure 3a), it is smaller (∼ 28 nm) in NDR/(PSS + Au NP) film (Figure 3c).

In the following section, the mechanical properties of the ultrathin inorganic/organic composite film were investigated mainly with the sensitive technique named strain-induced elastic buckling instability for mechanical measurements.[27,32] Just as shown in the ref 32a, spraying assembly of the Au NP/organic multilayer film was directly performed on a relatively soft and thick plasma-treated PDMS sheet (∼1 mm thick) with a hydrophilic surface. When the multilayer film-coated PDMS sheet was strained, an iridescent color of the assembly film appears because of the diffraction from the micrometer-scale periodic ridges produced (Figure S3). The film's elastic modulus is calculated via the a well-established buckling mechanics according to the following equation[27a]

$$E_f = \frac{3E_s(1 - V_f^2)}{1 - V_s^2}\left(\frac{\lambda}{2\pi d_f}\right)^3$$

where d is the thickness of the upper assembly film determined by AFM cross-section analysis, V is Poisson's ratio, λ is the buckling wavelength, and E is Young's modulus (subscripts f and s represent the film and substrate, respectively). The substrate of PDMS sheet used in the experiment has a Young's modulus of ∼1.3 MPa estimated with a microtesting method and a Poisson's ratio of 0.5 according to the reference value.[32a] For a PE/Au NP composite ultrathin film, the Poisson's ratio is assumed to be ∼0.4 because of PEs ultrathin film with a typical V of 0.33 in the dry state[32a] and Au film with V of ∼0.425.[40] Figure 4 demonstrates the buckling wavelength (λ) and the corresponding estimated Young's modulus of the composite films with different numbers of deposited bilayers. As expected from the above equation, the buckling wavelength is almost linearly related to the number of NDR/Au NP bilayers, also in agreement with the result of PEs multilayer films with no inorganic NP embedded.[32] The increment in the wrinkles' periodicity for each bilayer is ∼0.074 μm. The

(39) Dong, W.; Sukhorukov, G. B.; Möhwald, H. *Phys. Chem. Chem. Phys.* **2003**, *5*, 3003.

(40) Perrin, G. *J. Phys. Chem. Solids* **2001**, *62*, 2091.

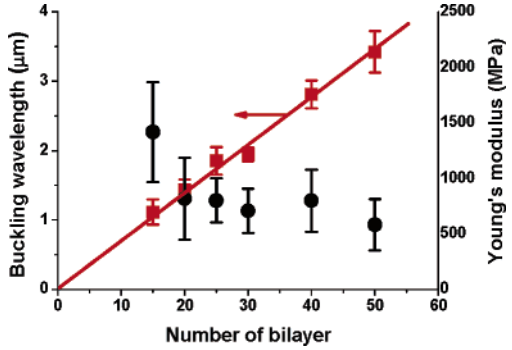

Figure 4. The buckling wavelength observed with optical microscopy and the estimated Young's modulus of $(NDR/Au\ NP)_n$ ultrathin film as a function of the number of assembled bilayers (n).

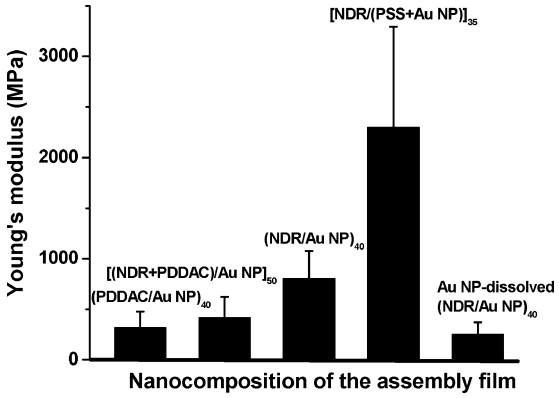

Figure 5. Effect of nanocomposition on the Young's modulus of the assembly films determined with the buckling test.

corresponding Young's moduli of the NDR/Au NP composite films are estimated to be 500−800 MPa.

Due to the influence of the PDMS substrate with a brittle SiOx-containing surface layer induced by plasma treatment,[32b,41] the thinner $(NDR/Au\ NP)_{15}$ film has a relatively higher Young's modulus.

To understand the effect of the composite's structure on the mechanical properties, we studied the Young's moduli of the films with adjustable compositions (Figure 5). These results clearly show that not only the structure and composition but also the elastic properties of the films can be tailored over a wide range by the coadsorption strategy. For the purpose of comparison, the Young's moduli of (PDDAC/Au NP) and Au NP-dissolved (NDR/Au NP) films have been given. Obviously, pure NDR/Au−NP films show an intermediate Young's modulus of ∼800 MPa. Coadsorption of NDR and PDDAC can reduce this value to ∼410 MPa. On the contrary, coadsorption of Au−NP and PSS leads to a dramatic increase to 2.3 GPa. Still, all the values are well above the range which could be explained by a pure rubberlike material. For this case, according to the ideal and simplest case of vulcanized rubber

$$E = 3\frac{\rho RT}{M}$$

a modulus of would be expected from the above equation.[42] Here, ρ/M, R, and T denote the density of cross-links, the ideal gas constant, and the absolute temperature, respectively. In our case, we expect a maximum cross-link density of ∼3450 mol·m^{-3} (crudely estimated) based on the mass density of the complex and the molecular weight of the NDR monomer. It is noted that the cross-linking density in LbL film is not so high because of the formation of a small degree of loops in the PE layers.[43] This estimated value of E is ∼25 MPa, well below the observed ones. Thus, under the conditions of the measurement, the covalent cross-linking has little effect on the mechanics. We observe the Young's modulus is in the following order: $E_{(PDDA/Au\ NP)40} < E_{[(PDD+NDR)/Au\ NP]35} < E_{(NDR/Au\ NP)40}$ with respect to the ionic bond-linked $(PDDAC/Au\ NP)_{40}$ film, partially cross-linking [(PDDAC + NDR)/Au NP]$_{35}$, and assumed fully cross-linked $(NDR/Au\ NP)_{40}$ films. Instead, the multilayers are mainly in a glassy state, and coadsorption allows for the change of organic matrix materials. On the other hand, the dissolution of the Au NP leads to the decrease of the Young's modulus of $(NDR/Au\ NP)_{40}$, suggesting the reinforcement of inorganic NPs on the mechanics. In our case, however, the Young's moduli of the as-prepared films are smaller than the reported value of PE films with only one Au NP interlayer embedded (5−10 GPa).[3] The reasons, we think, are related to the different mechanical characterization techniques and conditions (i.e., air humidity[32a]), film preparation method, and film compositions such as low average molecular weight of NDR used here (M_n −2100 g/mol). More importantly, the as-prepared films consist of 50−70 nm-sized nanoparticles with each one composed of 5-nm-sized Au NP and NDR (or PDDAC) (Figure 2 and 3a). Obviously, a continuous organic support is lacking in the as-prepared inorganic−organic composite films. This implies that introduction of an appropriate fraction of inorganic NP with uniform distribution in organic matrixes is more advantageous for the reinforcement of NP on the mechanical properties, such as the system of NDR/(PSS + Au NP) with a high elastic modulus of 2.3 GPa.

Conclusion

Photosensitive NDR/Au NP multilayer films with conveniently controlled nanostructures and good quality have been successively constructed with high efficiency through alternatively spraying the assembly solutions onto the vertically standing substrate, indicated by the characterization results of UV−vis spectroscopy and AFM. Subsequent UV irradiation leads to the formation of the covalently cross-linked composite film with an improved chemical stability, greatly broadening the flexible processing and the application field of the resultant functional films. On the other hand, the buckling test shows that the nanostructures of the composite films such as the organic matrix and the fraction of Au NPs are essential to adjust the mechanical properties. The obtained results allow us to design and synthesize advanced functional composite films with well-tuned mechanical properties and chemical stabilities.

(41) (a) Hillborg, H.; Tomczak, N.; Olah, A.; Schonherr, H.; Vancso, G. J. *Langmuir* **2004**, *20*, 785. (b) Hillborg, H.; Gedde, U. W. *Polymer* **1998**, *39*, 1991.

(42) Treloar, L. R. G. *The Physics of Rubber Elasticity*, 2nd ed.; Oxford Clarendon Press: Oxford, U.K., 1958; pp 187−196.

(43) Plunkett, M. A.; Claesson, P. M.; Ernstsson, M.; Rutland, M. W. *Langmuir* **2003**, *19*, 4673.

Acknowledgment. C.L. is grateful to the Alexander von Humboldt Foundation for a research fellowship. C.L. also thanks Professor Helmuth Möhwald for helpful discussions and supports, Professor Weixiao Cao for the present of NDR, and Dr. Ingo Burgert and Michaela Eder for their help in the measurement of the Young's modulus of the PDMS sheet.

Supporting Information Available: TEM image and UV spectrum of as-prepared Au NP (Figure S1), UV spectrum evolution after UV irradiation (Figure S2), and buckling test of composite films (Figure S3). This material is available free of charge via the Internet at http://pubs.acs.org.

CM061759Y